IOSR Journal of Applied Chemistry (IOSR-JAC)
e-ISSN: 2278-5736.Volume 13, Issue 3 Ser. I (March. 2020), PP 30-38
www.iosrjournals.org

Stem extract of *Dissotis theifolia* (Melastomataceae) as a green corrosion inhibitor for N80 steel in 1 M HCl solution

Nkem B. Iroha[1] and Maduelosi Ngozi Jane[2]
[1]*Electrochemistry and Material Science Unit, Department of Chemistry, Federal University Otuoke, Nigeria*
[2]*Department of Chemistry, Rivers State University, Port Harcourt, Nigeria*

Abstract: *The corrosion inhibition performance of stem extract of Dissotis theifolia (DT) on N80 steel corrosion in 1 M HCl solution has been studied using gravimetric method, electrochemical impedance spectroscopy (EIS), potentiodynamic polarization (PDP) and scanning electron microscopy (SEM). The stem extract of Dissotis theifolia is composed of tannins and flavonoids which are mainly responsible for the corrosion inhibition of the N80 steel. The results of the study reveal that DT inhibited the acid corrosion of N80 steel at different concentrations of the inhibitor. The inhibition efficiency increases with increasing concentration of the inhibitor with the maximum inhibition efficiencies of 94.1% obtained at 250 mg L^{-1} concentration. Polarization data show that the extract functioned via a mixed inhibition mechanism, affecting both the anodic and cathodic partial reactions of the corrosion process. EIS measurements revealed that the DT inhibits N80 steel corrosion by adsorbing on the steel surface. The adsorption of the inhibitor on the steel surface obeys Langmuir adsorption isotherm. The SEM images revealed the formation of protective film of the inhibitor on N80 steel surface.*

Keywords: *Corrosion inhibition, Dissotis theifolia, N80 steel, Polarization, Langmuir adsorption isotherm.*

Date of Submission: 26-02-2020 Date of Acceptance: 09-03-2020

I. Introduction

Materials deterioration due to corrosion is a major problem in petroleum industries and various mechanical, biochemical, metallurgical, and chemical engineering applications. Industrial processes such as oil-well acidizing, descaling, pickling etc. often involve mineral acids which usually causes serious surface corrosion and results in the material degradation and severe financial losses [1, 2]. It has been found that one of the best methods of protecting metals against corrosion involves the use of corrosion inhibitors [3]. However, the toxicity of inorganic and most organic corrosion inhibitors to the environment and humans has compelled the search for safer corrosion inhibitors called 'green corrosion' inhibitors due to their properties like non-toxicity, biodegradability, and low cost. The green inhibitors contain naturally occurring organic compounds and can be used as an alternative in etching and pickling solutions [4, 5].

Inhibitors are compounds that retard the rate of corrosion of metals by being adsorbed on the surface of the metal either through the transfer of charge from charge inhibitor molecule to charged metal surface (physical adsorption) or by electron transfer from the inhibitor's molecule to the vacant d-orbital of the metal(chemical adsorption) [6]. Most organic compounds containing polar functional groups, which could include heteroatoms and/or conjugated double bonds, exhibit excellent inhibition efficiency [7-9]. The efficacy of organic inhibitor compounds toward corrosion of metal in acid solution is directly associated with their adsorption properties. Various factors like nature of metal, chemical structure of inhibitor, presence of additives, testing media, solution temperature , solution concentration etc. influence adsorption of natural corrosion inhibitors on mild steel surface [10]. The effectiveness of natural products extracted from different plant parts toward corrosion inhibition has been reported by several authors [11–16].

Dissotis theifolia (DT) is a plant belonging to the family of Melastomataceae. The genus *Dissotis* comprises about 140 species, found in some African countries such as Nigeria, Democratic Republic of Congo, Ivory Coast, Benin, and Cameroon [17]. They are climbing shrubs, or small trees growing up to 2 m high with long, narrow leaves which are oppositely situated on the bract membranous stem with plain or finely saw-edges [18]. Extracts from the leaves, stem and roots of *D. theifolia* plant are used locally by communities in south eastern Nigeria to threat inflammations, wound, and sores. The stem of the plants are often converted to chewing stick to treat gum infections. The antibacterial property of *D. theifolia* against common bacteria pathogens has been studied [19] and the study also revealed that *D. theifolia* is rich in tannins and flavonoids. No previous studies have revealed the anticorrosion properties of DT. The present research investigates the green corrosion inhibitive behavior of DT on N80 steel in 1 M HCl solution using gravimetric, electrochemical

impedance spectroscopy (EIS) and potentiodynamic polarization (PDP) techniques. Surface analytical technique such as scanning electron microscopy (SEM) was used to observe the morphology of the N80 steel surface.

II. Material And Methods

Materials Preparation

N80 steel sheet of thickness, 0.2cm and composition (wt.%) C = 0.31, Mn = 0.92, P = 0.01, Si = 0.19, S = 0.008, Cr = 0.2 and the remainder Fe, was obtained from Shell Nigeria oil field. The N80 steel was cut into coupons of dimensions 4 cm x 1 cm for electrochemical measurements having 1 cm^2 unmasked surface and 3 cm x 2 cm for gravimetric and surface morphological studies. The coupons were mechanically polished with series of emery paper of grade 200, 400 and 600 grits, degreased with absolute ethanol, dried in acetone and preserved in desiccators prior to corrosion studies. 1 M HCl solution, prepared by diluting 37% HCl with double distilled water, was used as the corrodent.

The stems of *D. theifolia* were collected from a bush in Otuoke, Bayelsa State, Nigeria in April, 2019 and were authenticated in the herbarium of the Department of Botany, University of Port Harcourt, Nigeria. The plants parts were washed thoroughly with water, air-dried, pulverized, and weighed. Stock solution of the extract was made by soaking weighed amount of the previously grounded stems of DT in 1 M HCl solution and kept for 48 hours. From the stock solution, the filtrate was used to prepare a concentration range of 100 mg L^{-1} to 250 mg L^{-1}.

Gravimetric measurement

Gravimetric experiment was conducted by immersing the pre-weighed N80 steel coupons into test solutions in the absence and presence of different concentrations of DT for 5 h. Thereafter the samples were taken out, cleaned with distilled water, dried and weighed again accurately. All the tests were conducted in aerated 1 M HCl solution. The difference in the initial and final weight gives the value of the weight loss in 5 h. The experiments were repeated thrice, and the obtained average weight loss data were used to compute the corrosion rate (*CR*; mg cm^{-2} h^{-1}) as follows [20]:

$$CR = \frac{\Delta w}{At} \quad (1)$$

where Δw denotes the weight loss (mg), A represents the sample area (cm^2) and t symbolizes the exposure time (h). The percentage inhibition efficiency ($\%\eta_{WL}$) and the surface coverage (θ) were calculated from the *CR* values [21]:

$$\%\eta_{WL} = \left(\frac{CR_B - CR_I}{CR_B}\right) \times 100 \quad (2)$$

$$\theta = \frac{CR_B - CR_I}{CR_B} \quad (3)$$

where CR_B and CR_I represents the obtained corrosion rates in the absence and presence of DT.

Electrochemical measurements

All electrochemical measurements were performed using the electrochemical workstation (CH electrochemical analyzer model 604B, USA). The three electrode electrochemical cell assembly consists of N80 steel coupon as working electrode (WE), platinum rod as counter electrode (CE) and saturated calomel electrode (SCE) as reference electrode (RE) and containing 300mL of electrolyte. The temperature of the electrolyte was maintained at room temperature (30 ◦C). The electrochemical system was maintained in an unperturbed state for a period of 30 minutes in order to allow it to reach the steady open circuit potential (OCP) before each electrochemical measurement. The EIS measurements were carried out in a frequency range from 100 kHz to 0.01 Hz under potentiostatic conditions, with amplitude of 10 mV peak-to peak, using the AC signal at E_{corr}. The potentiodynamic polarization curves were obtained from −250 to +250 mV versus the open circuit potential (OCP), with a scan rate of 0.3 mV s^{-1}.

Scanning Electron Microscopy (SEM)

The surface morphology of the N80 steel specimens in the absence and presence of DT in 1 M HCl at 30°C were determined using Scanning Electron Microscopy. The N80 steel was immersed in uninhibited 1 M HCl solution and that containing optimum concentration of DT for 4 h immersion time. SEM images of inhibited and uninhibited steel specimens were recorded at 1000× using SEM model Zeiss Evo 50 XVP at the accelerating voltage of 15 kV.

III. Results and Discussion

Gravimetric measurements

Fig. 1a shows the plots of corrosion rate (CR) *vs.* Inhibitor concentration (η_{WL}) for the corrosion of N80 steel in 1 M HCl in the absence and presence of different concentrations of DT stem extract at different temperatures. The corrosion rate was observed to be lower in the presence of inhibitor than free acid solution and decreases with increase in the concentration of the inhibitor at the various temperature studied. Fig. 1b presents plot of inhibition efficiency *vs.* Inhibitor concentration (C_{inh}). From the plot (Fig. 1b) it can be seen that inhibition efficiency increased as the concentration of DT increases from (100 - 250) mg L^{-1}. The maximum inhibition efficiency of 94.1% was achieved at 250 mg L^{-1}. This behavior reflects the inhibitive effect of DT toward the acid corrosion of the steel, probably due to the adsorption of phytochemical constituents of the extract on the metal surface. It is well documented in literatures that increase in inhibitor concentration causes successive increase in surface coverage as the effectiveness of adsorption increases in the same order.

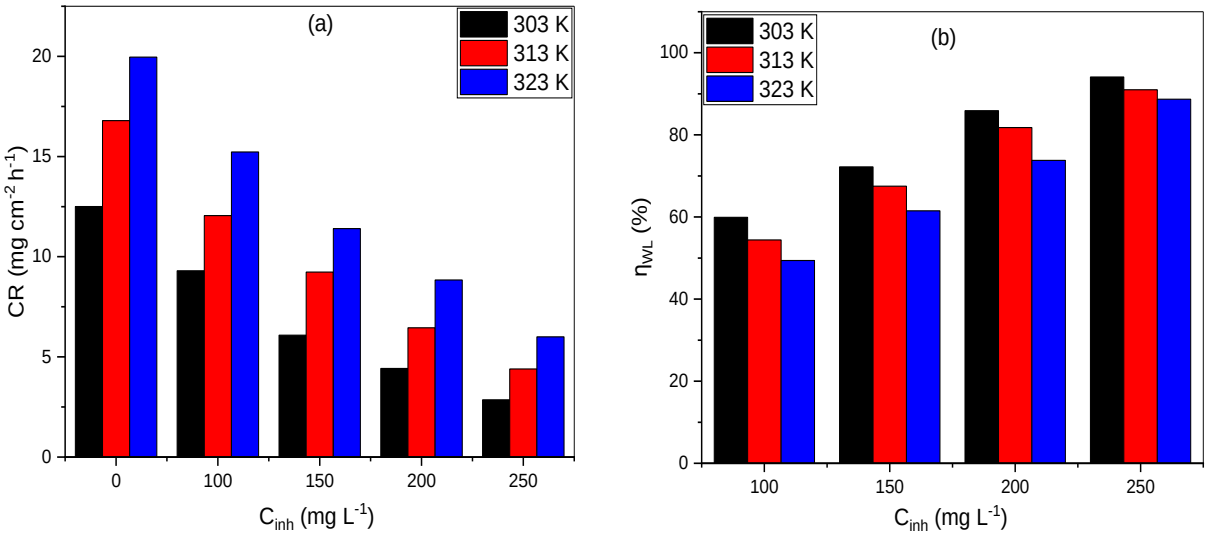

Fig. 1: Plots of (a) corrosion rate and (b) inhibition efficiency *vs.* Inhibitor concentration for N80 steel corrosion in 1 M HCl in the absence and presence of DT at different temperatures

Effect of temperature

The gravimetric studies were performed in the temperature range of 303 to 323 K at different concentrations of DT for studying the effect of temperature on the corrosion rate and inhibition efficiency. The results revealed that the rate of corrosion increases as the temperature increases and decreases as the concentration of DT increases. The relation between the corrosion rates (*CR*) of N80 steel in acidic media and temperature (T) is often expressed by the Arrhenius equation:

$$CR = A\exp\left(-E_a^*/RT\right) \qquad (4)$$

where E_a^* is the apparent activation energy, A is the Arrhenius pre-exponential factor and R is the universal gas constant. A plot of log *CR vs.* 1/*T* (Fig. 2a) gave straight lines with slope of $(-E_a^*/2.303R)$ at which the activation energies were calculated and listed in Table 1. It is seen in the table that the activation energies of DT inhibited acid solutions are bigger than those of uninhibited solutions. This means that, DT inhibited the steel corrosion by raising the energy barrier of the corrosion reactions and can be interpreted as due to physical adsorption [22, 23]. The other activation thermodynamic parameters of the corrosion reaction such as the enthalpy (ΔH^*) and the entropy (ΔS^*) of activation were determined using the transition state type equation [22, 24]:

$$CR = \left(RT/Nh\right)\exp\left(\Delta S^*/R\right)\exp\left(-\Delta H^*/RT\right) \qquad (5)$$

where *h* is the Planck's constant (6.62×10^{-34} Js), *N* is the Avogadro number (6.022×10^{23} mol^{-1}), *CR*, *T* and *R* retain their previous meaning. Plots of log (*CR*/*T*) *vs.* (1/*T*) gave a straight line with a slope of ($-\Delta H^*/2.303R$) and an intercept of [log (*R*/*Nh*) + $\Delta S^*/2.303R$], as shown in Fig.2b, from which the values of ΔH^* and ΔS^* were calculated and also listed in Table 1

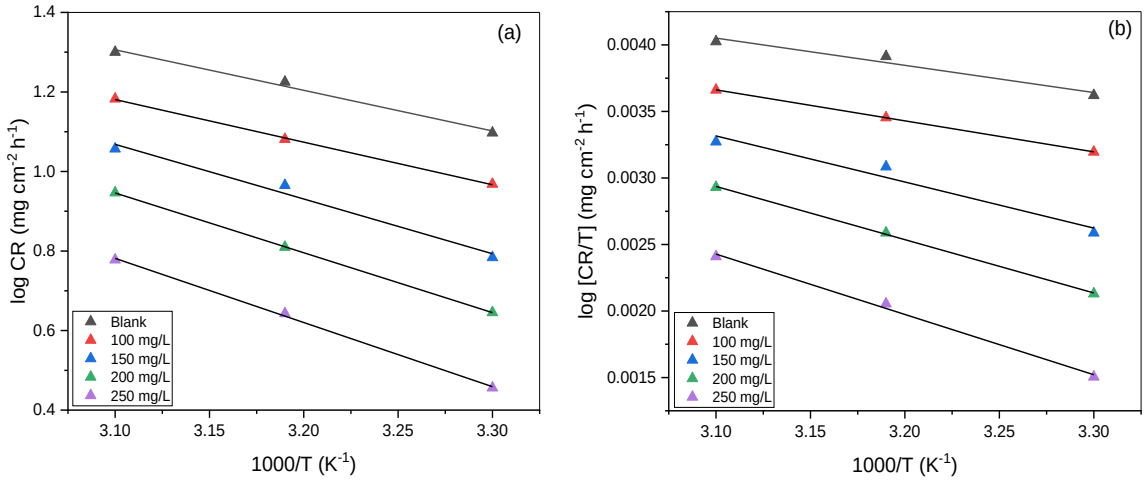

.

Fig. 2. (a) Arrhenius plots for N80 steel corrosion in 1 M HCl in the absence and presence of DT, (b) Transition state plots for N80 steel in 1 M HCl without and with various concentrations of DT

Table 1. Activation parameters for the dissolution of N80 steel in the absence and presence of different concentrations of DT stem extract in 1 M HCl

Concentration (mg L^{-1})	E_a **(kJ mol^{-1})**	ΔH^* **(kJ mol^{-1})**	ΔS^* **(J mol^{-1} K^{-1})**
Blank	69.27	30.35	-213.09
100	91.38	45.86	-218.43
150	101.90	49.23	-226.26
200	116.28	61.74	-236.97
250	122.14	74.52	-241.35

Table 1 show that value of enthalpy of activation, ΔH* is positive and higher in presence of inhibitor. The positive sign of ΔH* reflects the endothermic nature of the N80 steel dissolution process. Large and negative values of ΔS* imply that the activation stage of the adsorption process is controlled by associative interactions between the steel and the inhibitor molecules rather than dissociative formation of steel and water molecules [25].

Polarization Measurements

The potentiodynamic polarization curves for N80 steel immersed in 1 M HCl solution in the absence and presence of different concentrations of the DT after immersion for 30min at 30 ^{o}C are presented in Fig.3. It can be seen from Fig. 3 that the polarization curves shifted to either more cathodic or anodic region in the presence of the inhibitors compared to the blank acid system, showing that the studied DT stem extract inhibit the corrosion reaction. The polarization curves in the presence of DT show similar anodic and cathodic features as the blank, suggesting that the inhibitors do not change the mechanism of the anodic N80 steel dissolution in the acid as well as the cathodic hydrogen gas evolution associated with the corrosion process. The values of potentiodynamic polarization parameters such as corrosion potential (E_{corr}), corrosion current density (I_{corr}), cathodic and anodic Tafel slopes (βc, βa) were obtained from the polarization curves through extrapolation method and are listed in Table 2. Examination of the results in Table 2 shows that with the addition of inhibitors to the aggressive 1 M HCl solution, the values of I_{corr} decreases significantly with slight shift in the values of E_{corr} which indicates that DT molecules adsorb over the steel surface. The magnitude of the shift in E_{corr} is 51 mV which is less than 85 mV. Therefore, the studied DT stem extract can be classified as mixed-type inhibitors [26, 27]. The values of Tafel slopes βc and βa is slightly changed upon addition of DT as compared to blank, which implies that the DT molecules are blocking both cathodic and anodic sites resulting in an inhibition of the cathodic and anodic reactions [28, 29].The corrosion inhibition efficiency (%η_{PDP}) values were calculated and listed in Table 2, using the relation:

$$\%\eta_{PDP} = \left(\frac{I_{corr} - I_{corr(i)}}{I_{corr}} \right) \times 100 \qquad (6)$$

where I_{corr} and $I_{corr(i)}$ are the corrosion current density values in the absence and presence of inhibitor respectively. The obtained values presented in Table 2 reveal that %η_{PDP} increased with DT concentration.

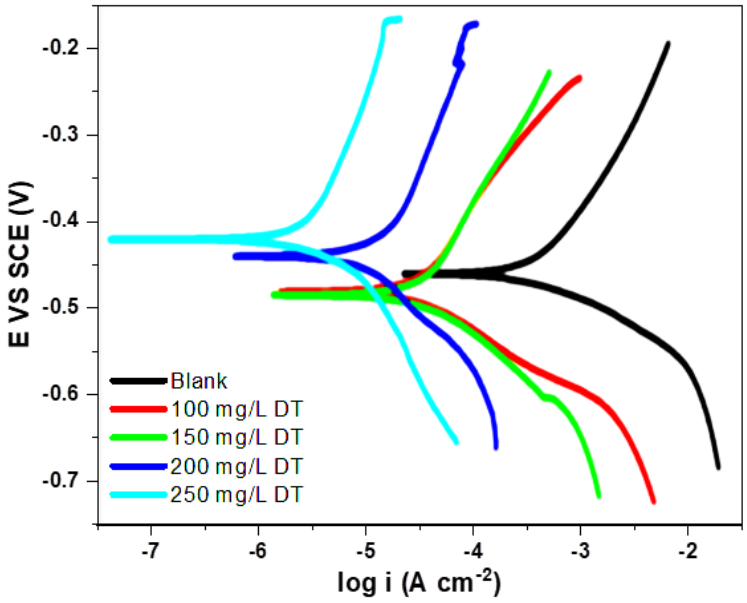

Fig. 3. Potentiodynamic polarization plots for N80 steel in 1 M HCl solution in the absence and presence of various concentrations of DT stem extract.

Table 2: Tafel polarization parameters for N80 steel in the absence and presence of DT stem extract inhibitor molecules in HCl medium

Concentration (mg L^{-1})	$-E_{corr}$ (mV vs SCE)	I_{corr} (μA cm^{-2})	b_a (mV dec^{-1})	b_c (mV dec^{-1})	η_{PDP} (%)
Blank	-471.8	1984	87.2	141.7	
100	-502.3	779	85.3	132.9	60.7
150	-519.5	458	90.5	118.0	76.9
200	-522.9	216	82.0	126.2	89.1
250	-520.1	103	78.4	125.8	94.8

Electrochemical impedance spectroscopy

The Nyquist plots obtained for the corrosion of N80 steel in the absence and presence of 100–250 mg L^{-1} inhibitor concentration are depicted in Fig. 4a. From the figure, it is seen that the Nyquist diagram displayed a single capacitive loop with shapes of depressed semicircles both in the inhibited and uninhibited 1 M HCl solutions. The semicircular size is larger in the inhibited solution and increases with the concentration of DT, suggesting that the inhibitor enhances the resistance of the N80 steel corrosion in the acid solution. The impedance kinetic parameters presented in Table 3 were determined by fitting the impedance data to the equivalent circuit model shown in Fig. 4b. The circuit comprises of a constant phase elements (CPE), a charge transfer resistance (R_{ct}) and a solution resistance (R_s). Generally, double layer formed by adsorption of inhibitors on the metallic surface behaves as CPE rather than pure capacitor. The capacitor is therefore replaced by CPE, which is a frequency dependent element and related to surface roughness, to fit the semicircle impedance data more accurately [30]. The impedance function of a CPE has the following equation [31]:

$$Z_{CPE} = Y_0^{-1}(j\omega)^{-n} \quad (7)$$

where the amplitude Y_0 and n are frequency-independent CPE constant and exponent, respectively, and ω is the angular frequency in rad s^{-1} for which $-Z_{max}$ reaches its maximum value, and $j^2 = -1$, an imaginary number, n is dependent on the surface morphology: $-1 \leq n \leq 1$.The values of the double layer capacitance (C_{dl}) were calculated from the R_{ct} values using the equation:

$$C_{dl} = \frac{1}{(2\pi f_{max} R_{ct})} \quad (8)$$

where f_{max} is the frequency value at which the imaginary component of the impedance is maximum ($-Z_{max}$). The inhibition efficiency ($\%\eta_{EIS}$) was calculated using the following relation [32, 33]:

$$\%\eta_{EIS} = \left(1 - \frac{R_{ct}}{R_{ct(i)}}\right) \times 100 \quad (9)$$

where R_{ct} and $R_{ct(i)}$ are the charge transfer resistances in the absence and presence of inhibitors respectively. The values of the C_{dl} and $\%\eta_{EIS}$ are also listed in Table 3.

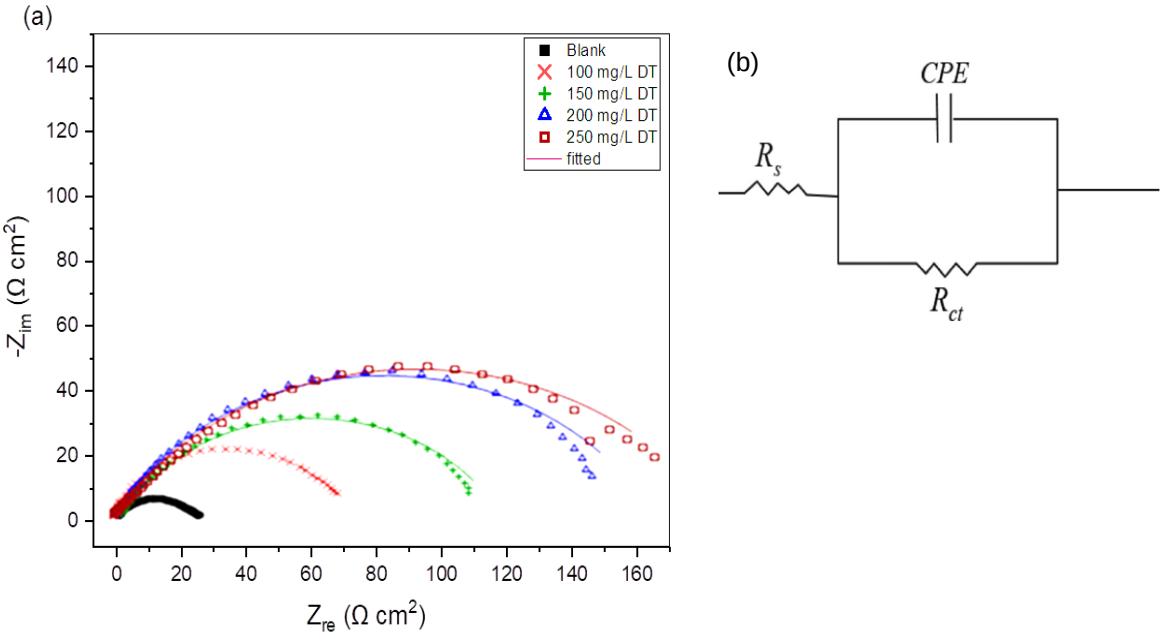

Fig. 4. (a) Nyquist plots of N80 steel in 1 M HCl without and with various concentrations of the DT stem extract (b) Schematic representation of equivalent circuit

Table 3. EIS parameters obtained for N80 steel in 1 M HCl in absence and presence of different concentrations of DT stem extract

Concentration (mg L^{-1})	R_s (Ω cm^2)	R_{ct} (Ω cm^2)	f_{max}	C_{dl} ($\mu F cm^{-2}$)	η_{EIS} (%)
Blank	0.985	9.65	27.5	600.0	
100	0.871	31.81	49.0	102.2	69.7
150	1.052	50.36	53.2	59.4	80.8
200	1.184	73.19	55.7	39.1	86.8
250	0.999	99.54	58.6	27.3	90.3

A careful inspection of the data in Table 3 reveals that the presence of different concentrations of the studied inhibitors increases the values of R_{ct} which could be as a result of increased surface coverage on N80 steel by the inhibitor molecules [31, 34]. In addition, the values of the C_{dl} in the presence of DT inhibitor are lower in comparison with the uninhibited values, which also suggest the adsorption of the inhibitor on the N80 steel surface leading to the formation of a protective layer. The corrosion inhibition efficiency ($\%\eta_{EIS}$) increases with increase in concentration of the inhibitor. The results show that the inhibition efficiencies obtained from the impedance study are in good agreement with those from gravimetric and polarization measurements.

Scanning Electron Microscopy (SEM)

Scanning electron microscopy images were taken to justify that the corrosion inhibition behavior of the studied DT stem extract is due to the formation of protective film on the steel surface. Fig. 5 shows the SEM images of N80 steel samples immersed in 1 M HCl without and with maximum concentration of the studied inhibitor after 4 h immersion time. The SEM image without inhibitor (Fig. 5a) is strongly corroded, resulting in a rough and heterogeneous surface of N80 steel in 1 M HCl. However, in the presence of the studied DT stem extract (Fig. 5b) the N80 steel surface is smoother and protected, which confirms their inhibition action [35].

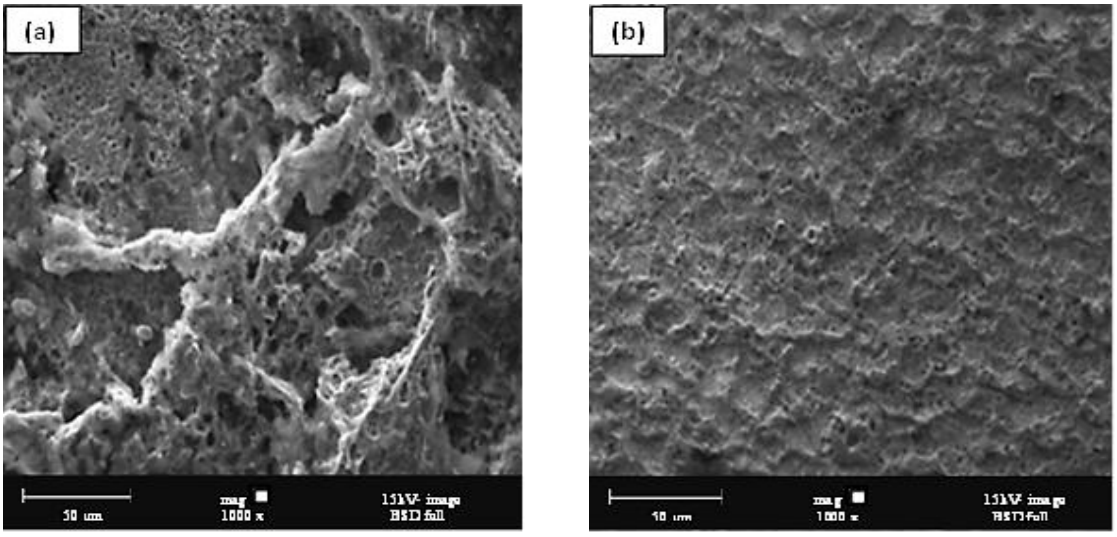

Fig. 5. SEM images of (a) N80 steel in 1 M HCl, (b) N80 steel in 1 M HCl + 250 mg L^{-1} DT

Adsorption isotherm

The establishment of adsorption isotherms that describe the adsorption of a corrosion inhibitor can provide important clues to the nature of the metal-inhibitor interaction. In order to acquire information about the adsorption of DT molecules on the N80 steel surface, the surface coverage values derived from the gravimetric results were used to test the best adsorption isotherm. The most frequently used isotherms include: Langmuir, Temkin, Frumkin, Flory-Huggins, Bockris-Swinkels and Dhar-Flory-Huggins. These adsorption isotherms were tested, and among them the Langmuir isotherm gave the best fit with values of regression coefficient (R^2) close to one. The Langmuir isotherm is represented by the following equation:

$$\frac{C_{inh}}{\theta} = \frac{1}{K_{ads}} + C_{inh} \qquad (10)$$

where, K_{ads} is the equilibrium constant of the adsorption-desorption process, θ is the degree of surface coverage and C_{inh} is molar concentration of inhibitor in the bulk solution. The adsorption isotherms for the DT stem extract are presented in Fig.6. The slight deviations of the slopes of the Langmuir plots from unity are due to the interactions between the adsorbed molecules on the metal surface as well as change in the heat of adsorption with increasing surface coverage. The values of K_{ads} were derived from the intercept ($1/K_{ads}$) and listed in Table 4.

Table 4. Adsorption parameters determined for DT studied as inhibitor of N80 steel corrosion in 1 M HCl

Temperature (K)	Slope	K_{ads} (mg^{-1} L)	R^2	ΔG^o_{ads} ($kJmol^{-1}$)
303	0.9425	0.0917	0.9916	-19.67
313	0.8810	0.0832	0.9899	-19.29
323	0.8307	0.0684	0.9901	-18.95

The adsorption equilibrium constant K_{ads} decreases with increase in experimental temperature, suggesting that the interactions between the adsorbed molecules and the N80 steel surface are weakened and consequently, the adsorbed molecules could become easily removable. K_{ads} is related to the standard free energy of adsorption, ΔG^0_{ads}, as follows:

$$\Delta G^0_{ads} = -RT \ln(55.5 K_{ads}) \qquad (11)$$

where R is universal gas constant (8.3147 $J.mol^{-1}.K^{-1}$), T is the absolute temperature (298 K) and 55.5 is the molar concentration of water in the solution. The calculated values of ΔG^0_{ads} at each studied temperature in presence of various concentration of DT are also given in Table 4. A negative ΔG^0_{ads} suggests that the adsorption of the inhibitor to the steel surface is spontaneous. The use of ΔG^0_{ads} values to describe the mode of adsorption of inhibitor molecules on metallic surface has been widely discussed [36, 37].

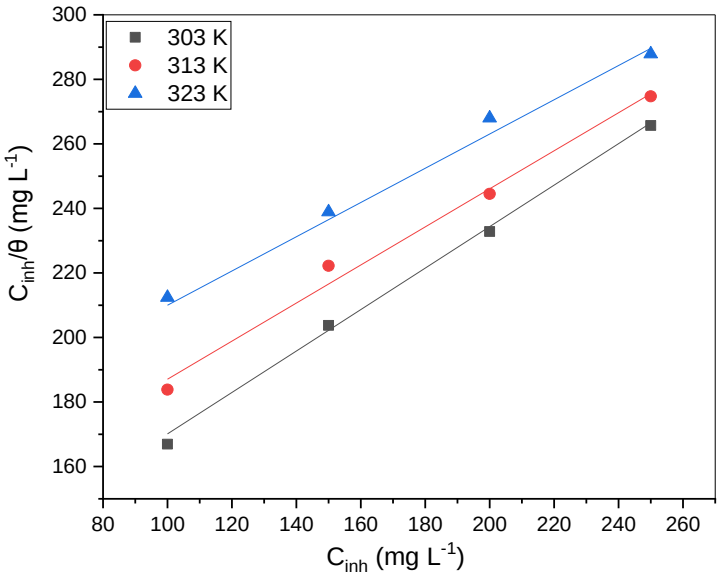

Fig. 6. Langmuir adsorption isotherms for the adsorption of DT on the N80 steel surface

The negative values of ΔG^0_{ads} indicate that the adsorption process is spontaneous and the adsorbed layer on the N80 steel surface is stable [38, 39]. Values of ΔG^0_{ads} are always used to classify adsorption process as physisorption (when ΔG^0_{ads} = −20 kJ mol^{-1} or less negative) or chemisorption (for ΔG^0_{ads} = −40 kJ mol^{-1} or more negative). The ΔG^0_{ads} values obtained in the present study range from −18.95 to −19.67 kJ mol^{-1}, which suggests that, the adsorption of the studied inhibitor on N80 steel surface is physisorption.

IV. Conclusion

In the present study, the corrosion inhibition performance of stem extract of *D. theifolia* was investigated for N80 steel in 1 M HCl using gravimetric and electrochemical methods and following conclusions were drawn:

(i) The *D. theifolia* was found to inhibit the corrosion of N80 steel in 1 M HCl and the inhibition efficiency increases with increasing concentration.

(ii) The adsorption of DT on the N80 steel surface was spontaneous and was consistent with physiosorption mechanism. The adsorption behavior of the DT inhibitor supported Langmuir adsorption isotherm model.

(iii) Impedance plots indicated that the charge transfer resistances increase with increasing concentration of the DT and maximum value was obtained at 250 mg L^{-1} concentration.

(iv) Potentiodynamic polarization measurements showed that the studied DT inhibitor is mixed type corrosion inhibitor.

(v) SEM analysis showed the reduction in damage of the Al in the presence of the inhibitor.

References

[1] Keles H., Keles M., Dehri I., Serindag O., The inhibitive effect of 6-amino-m-cresol and its Schiff base on the corrosion of mild steel in 0.5M HCl medium. *Materials Chemistry and Physics*, 2008; 112:173-179.

[2] Iroha N. B. and Hamilton-Amachree A., Adsorption and anticorrosion performance of Ocimum Canum extract on mild steel in sulphuric acid pickling environment, *American Journal of Materials Science*, 2018; *8(2)*, 39-44

[3] Ali S. A., Saeed M. T., Rahman S. V., The isoxazolidines: a new class of corrosion inhibitors of mild steel in acidic medium, *Corrosion Science*, 2003; 45(2):253–266

[4] Banerjee S., Srivastava V, Singh M.M. Chemically modified natural polysaccharide as green corrosion inhibitor for mild steel in acidic medium. *Corrosion Science*. 2012;59:35–41.

[5] Iroha N. B, Chidiebere M. A., Evaluation of the Inhibitive Effect of Annona Muricata. L Leaves Extract on Low-Carbon Steel Corrosion in Acidic Media, *International Journal of Materials and Chemistry*, 2017;7(3):47-54.

[6] Ameh P.O, Eddy N.O. *Commiphora pedunculata* gum as a green inhibitor for the corrosion of aluminium. *Res Chem Intermed* 2014;40(8):2641–9.

[7] Varvara S., Bostan R., Bobis O., Gaina L., Popa F., Mena V., Souto R.M. Propolis as a Green corrosion inhibitor for bronze in weakly acidic solution, *Appl. Surf. Sci.* 2017;426:1100-1112.

[8] Saxena A., Prasad D., Haldhar R., Singh G., Kumar A. Use of Sida cordifolia extract as green corrosion inhibitor for mild steel in 0.5M H_2SO_4, *J. Env. Chem.Eng.* 2018;6:694-700.

[9] Xiong J., Grant Chen D.K.X. Superhydrophobic honeycomb-like cobalt stearate thin films on aluminium with excellent anti-corrosion properties, *Appl. Surf. Sci*. 2017;407:361-370.

[10] Verma C, Quarishi M.A, Adsorption behaviour of 8,9 –bis (4 (dimethyl amino) phenyl) benzo (4,5) imidazo(1,2 –a) pyridine-6,7 –dicarbonitrile on mild steel surface in 1 M HCl. *J. Assoc. Arab Univ. Basic Appl. Sci.* 2017;22:56 – 61.

[11] El-Taib Heakal, F., Deyab, M.A., Osman, M.M., Elkholy, A.E, Performance of *Centaurea cyanus* aqueous extract towards corrosion mitigation of carbon steel in saline formation water. *Desalination* 2018; 425:111–122.

[12] Iroha N. B, Madueke N. A., Effect of *Triumfetta rhomboidea* Leaves Extract on the Corrosion Resistance of Carbon Steel in Acidic Environment, *Chemical Science International Journal, 25(2),* 2018, 1-9.

[13] Shalabi, K., Abdallah, Y. M., Hala, M. H. and Fouda, A. S. Adsorption and corrosion inhibition of *atropa belladonna* extract on carbon steel in 1M HCl solution. *International journal of electrochemical science*, 2014; 9:1468-1487.

[14] Oguzie E., Onuoha G., Ejike E., Effect of *Gongronema latifolium* extract on aluminium corrosion in acidic and alkaline media", Pigment Resin Technology, 2007;36(1), 44-49.

[15] Okafor P.C., Ebenso E.E, Ekbe U.J. *Azadirachta indica* extracts as corrosion inhibitor for mild steel in acidic medium, *International Journal of Electrochemical Science*, 2010;5(7):978-993.

[16] Li X., Deng S., Fu H., Inhibition of the corrosion of steel in HCl, H_2SO_4 solutions by bamboo leaf extract, *Corrosion Science*, 2012;62:163-175.

[17] Loigier H. A., Descriptive flora of Puerto Rico and Adjacent islands. *Eds*., 2009;8:113–115

[18] Harold N.S., A handbook of West African Flowers, London: Oxford University Press, 1966; p. 27

[19] Ofokansi K.C, Adikwu M.U, Esimone, C.O, Nwodo M. *In vitro* evaluation of the combined antibacterial activity of the leaf extracts of *Dissotis theifolia* with some disc antibiotics. *Indian J. Pharm. Sci*. 2004; 66(5): 659-664.

[20] Madueke N. A., Iroha N. B., Protecting aluminium alloy of type AA8011 from acid corrosion using extract from Allamanda cathartica leaves, *International Journal of Innovative Research in Science, Engineering and Technology*, 2018;7(10):10251-10258

[21] Iroha N. B., Akaranta O., James A. O., Red onion skin extract-furfural resin as corrosion inhibitor for aluminium in acid medium, *Der Chemica Sinica*, 2012;*3(4):* 995-1001.

[22] Tao Z., He W., Wang S., Zhang S., Zhou G., A study of differential polarization curves and thermodynamic properties for mild steel in acidic solution with nitrophenyltriazole derivative. *Corrosion Science*, 2012;60:205–213.

[23] *Adsorption of Molecules at Metal Electrodes*, Lipkowski, J.and Ross, P., Eds., New York: VCH, 1992.

[24] Solomon M.M., Gerengi H., Umoren S.A., Carboxymethyl cellulose/silver nanoparticles composite: synthesis, characterization and application as a benign corrosion inhibitor for St37 steel in 15% H2SO4 medium. *ACS Appl. Mater. Interfaces*, 2017;9:6376–6389.

[25] Mourya P., Singh P., Tewari A. K., Rastogi R. B., Singh M. M. Relationship between structure and inhibition behaviour of quinolinium salts for mild steel corrosion: Experimental and theoretical approach. *Corrosion Science*, 2015;95:71–87.

[26] Chidiebere M. A., Simeon N., Njoku D., Iroha N. B., Oguzie E. E. and Li Y., Experimental study on the inhibitive effect of phytic acid as a corrosion inhibitor for Q235 mild steel in 1 M HCl environment, *World News of Natural Sciences, 15*, 2017, 1-19.

[27] Ferreira, E. S., Giancomelli, C., Giacomelli, F. C., Spinelli, A. Evaluation of the inhibitor effect of l-ascorbic acid on the corrosion of mild steel. *Mater. Chem. Phys.*, 2004;83:129–134.

[28] Chauhan L.R., Gunasekaran G. Corrosion inhibition of mild steel by plant extract in dilute HCl medium. *Corrosion Science*, 2007;49:1143-1161

[29] Ahamad I., Prasad R., Quraishi M.A. Adsorption and inhibitive properties of some new Mannich bases of Isatin derivatives on corrosion of mild steel in acidic media. *Corrosion Science*, 2010;52:1472.

[30] Yadav D. K., Quraishi M. A., Electrochemical investigation of Substituted Pyranopyrazoles Adsorption on Mild Steel in Acid Solution, *Ind. Eng. Chem. Res.* 2012;51:8194–8210

[31] Hamilton-Amachree A., Iroha, N. B. Corrosion inhibition of API 5L X80 pipeline steel in acidic environment using aqueous extract of *Thevetia peruviana*. *Chemistry International*, 2020;6(3):117-128.

[32] Roy P., Karfa P., Adhikari U., Sukul D., Corrosion inhibition of mild steel in acidic medium by polyacrylamide grafted Guar gum with various grafting percentage: Effect of intramolecular synergism *Corrosion Science*., 2014;88:246–253.

[33] Iroha N. B., Hamilton-Amachree A., Inhibition and adsorption of oil extract of Balanites aegyptiaca seeds on the corrosion of mild steel in hydrochloric acid environment, *World Scientific News*, 2019;126:183-197.

[34] Zheng X , Zhang S , Li W , Gong M , Yin L . Experimental and theoretical studies of two imidazolium-based ionic liquids as inhibitors for mild steel in sulfuric acid solution, *Corrosion Science*, 2015;95:168–179

[35] Yadav, D. K.; Chauhan, D. S.; Ahamad, I.; Quraishi, M. A. Electrochemical Behavior of Steel/Acid Interface: Adsorption and Inhibition Effect of Oligomeric Aniline. *RSC Adv*.2013, 3, 632−646.

[36] Olasunkanmi L. O., Kabanda M. M., Ebenso E. E., Quinoxaline derivatives as corrosion inhibitors for mild steel in hydrochloric acid medium: Electrochemical and quantum chemical studies. *Physica E* 76;2016:109–126

[37] Obot I. B., Obi-Egbedi, N. O. Adsorption properties and inhibition of mild steel corrosion in sulphuric acid solution by ketoconazole: Experimental and theoretical investigation. *Corrosion Science*, 52;2010:198–204.

[38] Iroha N. B., James A. O., Assessment of performance of velvet tamarind-furfural resin as corrosion inhibitor for mild steel in acidic solution, *J. Chem Soc. Nigeria*, 43(3);2018:510–517.

[39] Cang H., Fei Z., Shao J., Shi, W. Xu Q. Corrosion Inhibition Of Mild Steel By Aloes Extract In Hcl Solution Medium. *Int. J. Electrochem. Sci.*, 8;2013:720-734

Nkem B. Iroha,etal. "Stem extract of Dissotis theifolia (Melastomataceae) as a green corrosion inhibitor for N80 steel in 1 M HCl solution." *IOSR Journal of Applied Chemistry (IOSR-JAC)*, 13(3), (2020): pp 30-38.